Acta Polytechnica **65**(4):429–441, 2025
https://doi.org/10.14311/AP.2025.65.0429

Published by the Czech Technical University in Prague

SIMULATION OF AN ACTIVE COOLING SYSTEM FOR LOW-CONCENTRATING PHOTOVOLTAIC SOLAR CELLS

Sayat Orynbassar, Ainur Kapparova, Gulbakhar Dosymbetova*, Dinara Almen, Evan Yershov, Ahmet Saymbetov, Madiyar Nurgaliyev, Batyrbek Zholamanov

Al-Farabi Kazakh National University, Faculty of Physics and Technology, 71 Al-Farabi, 050040 Almaty, Kazakhstan

* corresponding author: dossymbetova.g@kaznu.kz

Abstract. One of the key challenges of concentrating photovoltaic (CPV) systems is the need for effective thermal management, as the increased solar irradiance significantly raises the operating temperature of solar cells, thereby reducing their efficiency. This study proposes a passive cooling solution for a Π-shaped low-concentration photovoltaic (LCPV) system, designed without a mechanical pump and uses gravity-fed water circulation. The thermal performance of the system was analysed using COMSOL Multiphysics. The simulation results demonstrate that the developed cooling system achieves high temperature uniformity, with a maximum surface temperature difference of only 0.07 °C for a radiator comprising five tubes. The system is capable of reducing the solar cell temperature from 40 °C to 22 °C in 10 seconds. Various radiator configurations were investigated for a module consisting of nine solar cells, confirming that the proposed system enables rapid cooling and maintains the cell temperature within optimal operating conditions. The presented design offers a simple, energy-efficient, and cost-effective solution for thermal regulation in LCPV modules.

Keywords: Water-cooling system, cooling time, LCPV, concentration ratio, heatsink.

1. Introduction

Traditional sources of electricity have a significant negative impact on the environment and to tackle the issue, renewable energy sources, such as solar energy, are an environmentally friendly solution [1]. However, the overall costs of generating solar power remain high, despite a rapid decline in solar technology costs in recent years [2]. The efficiency of PV panels is also considered to be lower, and their performance is influenced by a number of factors.

Over the past decade, the global photovoltaic (PV) sector has grown rapidly in response to the urgent need to reduce carbon emissions and mitigate global warming. By 2023, the total installed PV capacity worldwide reached an estimated 1.6 TW, with China and the United States being the largest contributors, accounting for approximately 760 GW and 265 GW of the capacity, respectively. At the same time, installing PV systems in Africa has shown significant progress, reaching nearly 221 GW. This substantial growth reflects the increasing demand for sustainable energy solutions and highlights the importance of developing more efficient and affordable PV technologies to support further growth of the global solar energy market [3].

The development of PV solar energy fields plays a crucial role in expanding the share of clean energy worldwide. Large-scale PV installations are especially important as they can effectively complement both renewable and conventional energy sources in hybrid energy systems. Such hybrid systems, including combinations such as PV/grid, PV/wind, PV/diesel, and PV/concentrated solar power, as well as more complex configurations such as PV/wind/diesel and PV/wind/battery, are widely implemented around the world. These integrated solutions provide greater reliability and flexibility in power generation by utilising diverse energy resources, which enhances the overall stability of the system and helps to meet the growing electricity demands in a sustainable way [4–9].

Recent practical projects demonstrate the various ways in which photovoltaic solar energy is being used to meet modern energy demands. One notable example is the implementation of stand-alone solar PV systems for urban street lighting, as shown by the case study of a roundabout in Kuwaiti in the Gaza Strip, where various off-grid configurations were designed to power advanced LED street lights with automatic controls, improving sustainability and energy efficiency of urban infrastructure [10]. Another significant project is the development of a 14 MW grid-connected PV power plant in Hoon City, Libya, which, using polycrystalline silicon technology, delivers over 24 964 MWh of clean electricity annually with a high average performance ratio of 76.9 % [11]. In addition, innovative concepts such as modular open-source solar DC nanogrids are being introduced to enable flexible, stand-alone power supply for different voltage levels, supported by efficient energy management systems that adapt to varying generation and load conditions – making solar power more accessible, especially for

isolated communities [12]. Together, these examples demonstrate the wide-ranging potential of PV technology to address energy needs at different scales and in different contexts.

Firstly, an increase in solar irradiance leads to an increase in the electrical power output of a PV panel, as the solar irradiance and the current of a PV panel have a linear relationship [13]. To increase the incident solar irradiance, concentrating optics, such as mirrors, lens, and other concentrating elements are used for the surface of the solar cells [14]. Using concentrating optics increases the solar radiation by collecting the sunlight into a small surface. Increased solar radiation improves the electrical efficiency of the CPV system. Moreover, concentrated PV panels use less area compared to photovoltaic panels [15]. CPV systems can be divided into three categories according to their level of concentration: low, medium, and high concentrating photovoltaics [16]. Low concentrating photovoltaics are the cheapest CPV systems and can have various designs [17]. In the paper [18], the authors achieved an electrical and thermal efficiencies of 28 % and 54 %, respectively, demonstrating that the overall efficiency of the system can be more than 80 % for a point-focus Fresnel-lens high-concentrating photovoltaic system. The work done by us [19] proved that a polycrystalline-silicon Fresnel-based low-concentrating photovoltaic system can increase the generated electrical energy by 27 %.

Secondly, although concentrating optics can increase the intensity of incident sunlight, high solar radiation leads to an increase in the temperature of a solar cell [20]. A solar cell converts approximately less than 20 % of the irradiance into electrical energy, while the rest is converted into heat. The temperature of the solar cell has a great influence on the behaviour of a PV system, as it greatly affects the system efficiency and energy output. An increase in cell temperature leads to the decrease in the open circuit voltage, with the two having a linear relationship [21]. Moreover, the temperature increase of a solar cell might affect its lifespan and reduce its performance [22]. CPV cells exhibit degradation at long duration high temperatures [23]. Therefore, to overcome the effects of cell temperature and keep the solar cell at normal temperature, a cooling system has to be developed [24]. In CPV systems, the temperature of a solar cell can exceed 100 °C, depending on the concentration ratio of the system. However, depending on the types and the structure of the solar cells, their normal working temperature may differ. Some highly efficient multi-junction solar cells can withstand high temperatures and do not show degradation, but the multi-junction solar cells are much more expensive than crystalline silicon solar cells [25]. One of the cheapest solar cells is a single-junction crystalline silicon solar cell. In the paper [26], the authors showed that the maximum output power decreased by 0.66 % with an increase of 1 K in the operating temperature of the crystalline silicon solar cell, therefore, it is necessary to improve the cooling methods for concentrated silicon solar cells.

There are several types of cooling methods and generally, they are classified as passive and active cooling techniques [27]. Currently, the most common cooling techniques for CPV systems include heat pipe cooling, water cooling, liquid immersion cooling, microchannel heat sink cooling, and phase-change material systems. However, there is no single best cooling method, as each of them has its advantages and disadvantages [23]. With an active cooling system, we can get a more uniform distribution of solar cell temperature than with passive cooling [28]. The most frequently used passive cooling systems are PCM-based (Phase-change materials) techniques, followed by air-based, liquid-based (e.g. water and nanofluids), and finally, radiative based techniques [29]. A major drawback of passive cooling systems is that the cooling area is proportional to the degree of concentration. Therefore, for a CPV system, a large area for heat dissipation is necessary [30]. It is proved that the Convective Heat Transfer Coefficient (CHTC) of active cooling systems is much higher than that of passive cooling systems. The CHTC of water is between 200 and 1 000, whereas the CHTC of air is between 1 and 10 under natural convection, which is much lower than that of water. Therefore, the cooling rate is higher with water than with air [31].

In paper [20], the authors designed an LCPV system with 8.5 Suns and an active water-cooling system. As a result, the output power was increased by a factor of 4.7 to 5.2, depending on the water flow rate, compared to a PV system without cooling. In the work done by us [32], we showed one of the ways to improve the performance of water-cooled LCPV systems using NN. In the paper [33], the authors concluded that the output from a CPV with a cooling system is 4.7 to 5.2 times higher than that from a fixed PV module. In the paper [34], the authors studied the influence of flow rate on the water-cooling process. The cooling system with a buried water heat exchanger successfully reduced the temperature of a solar panel with a V-trough concentrator from 72.5 °C (without cooling) to 47.2 °C, 45.5 °C, 41.8 °C and 39.3 °C, at water cooling flow rates of 0.01 $\mathrm{kg\,s^{-1}}$, 0.02 $\mathrm{kg\,s^{-1}}$, 0.03 $\mathrm{kg\,s^{-1}}$ and 0.04 $\mathrm{kg\,s^{-1}}$, respectively. In addition, the peak generated electrical power increased by 18.6 %, 20.9 %, 23.5 % and 28.3 % compared with that of the uncooled panel at water cooling flow rates of 0.01 $\mathrm{kg\,s^{-1}}$, 0.02 $\mathrm{kg\,s^{-1}}$, 0.03 $\mathrm{kg\,s^{-1}}$ and 0.04 $\mathrm{kg\,s^{-1}}$, respectively. The electrical and thermal efficiencies increased with increasing cooling water flow rates.

Also, the water cooling performance depends on the design of the cooling system. Authors of the work [35] introduced different designs of cooling pipes on the backside of a PV module to find the effect of pipe geometries on the performance of PV modules and proved that using a cooling pipe for each string significantly improves the electrical efficiency of the PV cells.

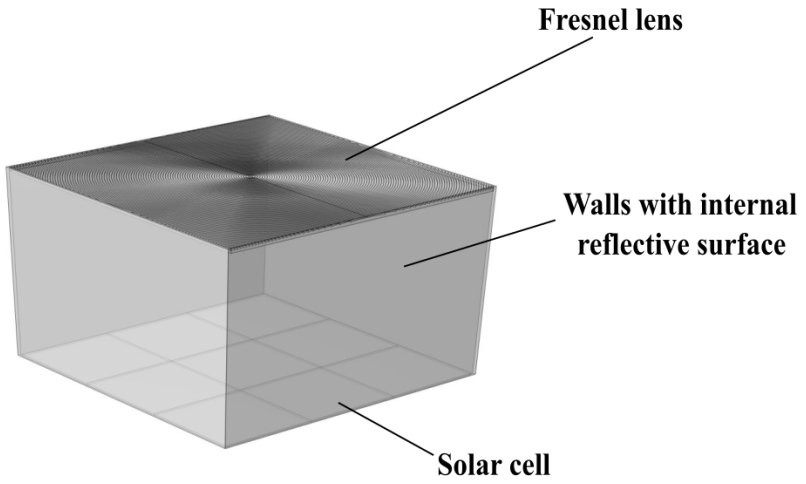

FIGURE 1. The Π-shaped optical system based on Fresnel lens and reflective surface with nine solar cells.

In paper [36], the authors developed a water-cooling system for LCPV based on reflectors in, which the pipes are located under each string. Compared to CPV without cooling. the maximum electrical increased efficiency from 15.88 % to 17.55 %. In the paper [37], when the number of water pipes increased from 2 to 6, the electrical and thermal efficiencies increased, and their variation became in the range of 8.05 to 8.96 % and 46.8 to 63.2 %, respectively. Thereby, the location and quantity of pipes can improve the performance of a water-cooling system.

In this work, we proposed and analysed an active water-cooling system design for a Π-shaped LCPV module, which integrates a Fresnel lens and four mirrors to ensure uniform solar irradiance. The main objective is to investigate the performance of a water-cooling system with copper tubes, examining how varying the number of tubes affects heat removal when each solar cell is cooled individually. The system is modelled and simulated using COMSOL Multiphysics to evaluate its thermal behaviour. In one of our previous studies, we developed a detailed optical model of the same LCPV configuration in COMSOL Multiphysics, calculated its electrical output, and analysed thermal management strategies [38]. A key advantage of the proposed design is its passive circulation: water flows by gravity from a certain height without the need for a pump, which reduces system complexity and energy consumption. The novelty of this work lies in achieving a uniform temperature distribution by optimising the number of tubes and ensuring that each solar cell is cooled separately. The results demonstrate that increasing the number of tubes significantly improves temperature uniformity and reduces the cooling time. For example, a radiator with five tubes exhibits a minimal temperature difference between its hottest and coolest points, confirming stable thermal performance. Overall, the proposed cooling concept can maintain favourable operating temperatures, contributing to consistent energy generation and extending the lifespan of the solar cells.

Parameter	Value
Size of the Fresnel lens [mm^2]	150×150
Size of the solar cell [mm^2]	52×52
Reflective coefficient of mirror	1
The material of Fresnel lens	Silica glass
Thickness of Fresnel lens [mm]	2

TABLE 1. Parameters of the Π-shaped optical system.

2. Design of the water-cooling system

The performance of a cooling system is primarily determined by the number of pipes and its design. In this study, the cooling system is designed for a Π-shaped LCPV system with nine polycrystalline silicon solar cells. The optical configuration, as shown in Figure 1, consists of a Fresnel lens and four reflective surfaces. The concentration ratio of the optical system can range between 2 and 8 depending on the length of the reflective surfaces. The system includes nine solar cells that allow for inclined incident rays. In this case, a non-uniform temperature distribution can occur; therefore, it is necessary to apply a cooling system that can uniformly cool the entire system within a short period of time. The main optical parameters of the Π-shaped LCPV system are summarised in Table 1.

The cooling system operates according to the following principle: the water tank is installed at a certain height, allowing water to be delivered by gravity to the water distributor, which then distributes it to the cooling radiators installed in each Π-shaped optical system. The distributor controls the water supply to each solar cell individually, based on temperature monitoring. Next, the water flows from one optical system to the next, repeating the described process. The used water at the outlet of the entire system is then pumped back to the tank.

The cooling system, shown in Figure 2, consists of a water storage tank, water distributor, and a system

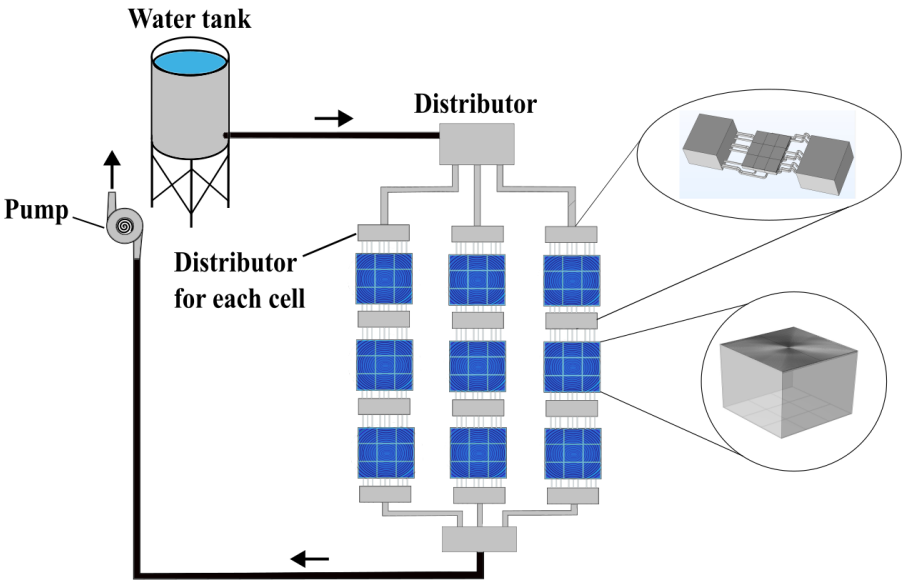

Figure 2. The cooling system.

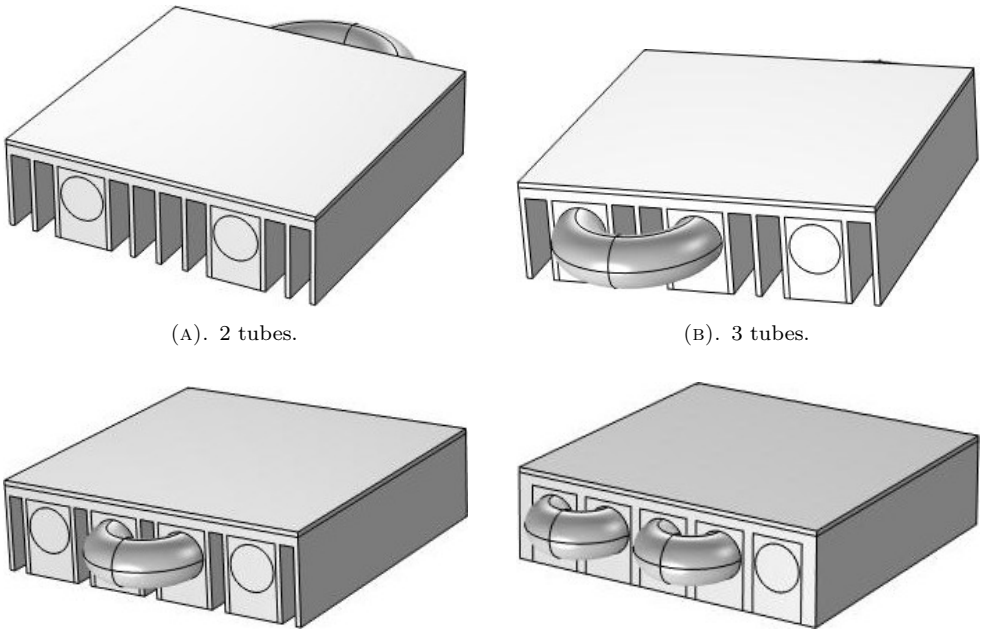

(a). 2 tubes. (b). 3 tubes.

(c). 4 tubes. (d). 5 tubes.

Figure 3. Heatsinks with 2, 3, 4, and 5 tubes.

consisting of 9 cooling radiators and a water pump. Cooling systems with 2-tube, 3-tube, 4-tube, 5-tube radiators were proposed for cooling the concentrated solar cell (Figure 3).

Figure 4 shows a system consisting of 9 cooling radiators with a height of 15 mm. A water dispenser is installed in the inlet part of the system. The device does not have a special water pump or active devices, which force the water to move forwards. Figure 3b shows an aluminium radiator for one solar cell, measuring 50 × 50 mm. The cooling system consists of 9 electro-valves, 9 temperature sensors, and a microcontroller.

With the help of temperature sensors installed on each radiator, the microcontroller makes decisions about opening and closing the valves according to the algorithm shown in Figure 4.

It is important to determine the most optimal arrangement of water pipes in radiators for cooling, therefore, according to the order of arrangement: 1 input – 1 output, 3 input – 3 output, 9 input – 9 output options were proposed.

Copper tubes with a diameter of 9 mm were installed in the radiator for water distribution. Based on many experiments and articles, it was found that the most common metals used in cooling are aluminium and copper. It was also found that their thermal conductivity is high. In general, it should be noted that such a cooling unit is easy to make and its components are easy to find.

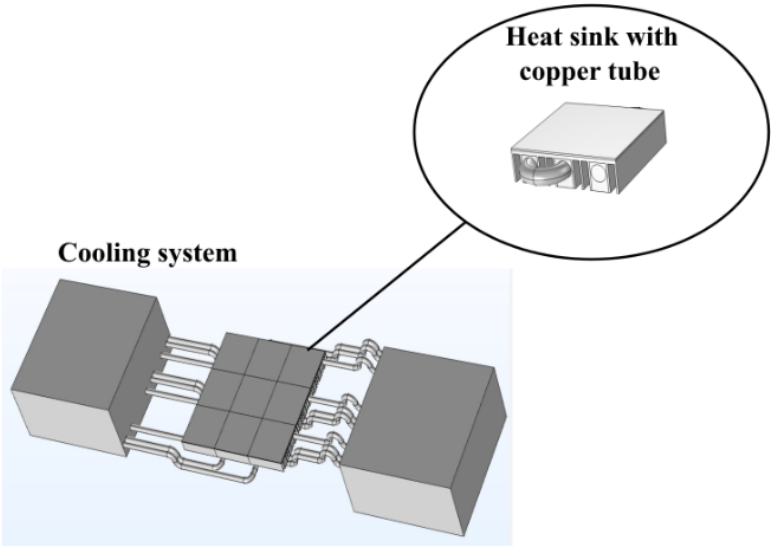

FIGURE 4. Water-cooling system design for concentrated solar cells.

Figure 5 shows the flow diagram of the water dispenser in the cooling system. When the temperature of one solar cell is higher than the threshold temperature, the valve corresponding to that solar cell opens and water flows through it.

The proposed active water-cooling system was analysed using a three-dimensional Multiphysics model in COMSOL to assess the thermal performance and cooling efficiency under varying solar radiation levels. The simulation approach integrates multiple physical phenomena, specifically fluid dynamics, heat transfer, and radiative heat exchange, to realistically represent the heat removal process within a cooling radiator.

Geometrical modelling and domain assumptions: The cooling radiator and flow channels were modelled as solid copper tubes, embedded within an aluminium heat sink geometry. The solar cell surface was defined as the heat source exposed to incident solar radiation, assumed to be perpendicular to the surface for maximum absorption. The model assumes a steady inlet flow with fully developed laminar flow conditions inside the tubes. The working fluid (water) is treated as incompressible and Newtonian.

Governing physical processes: The fluid flow inside the tubes is governed by the Navier-Stokes equations under laminar flow assumptions due to the moderate Reynolds number corresponding to the given flow velocity. The heat transfer between the solid radiator and the flowing water is modelled using the standard energy conservation equation, accounting for conduction in solids and combined conduction-convection in fluids. Surface-to-surface radiation is included to simulate the thermal exchange between exposed surfaces within the cooling module and to represent the absorption of incident solar irradiance.

Multiphysics coupling: The Non-isothermal Flow interface couples the velocity and pressure fields of the liquid with the temperature distribution, ensuring that the convective heat transfer is correctly resolved.

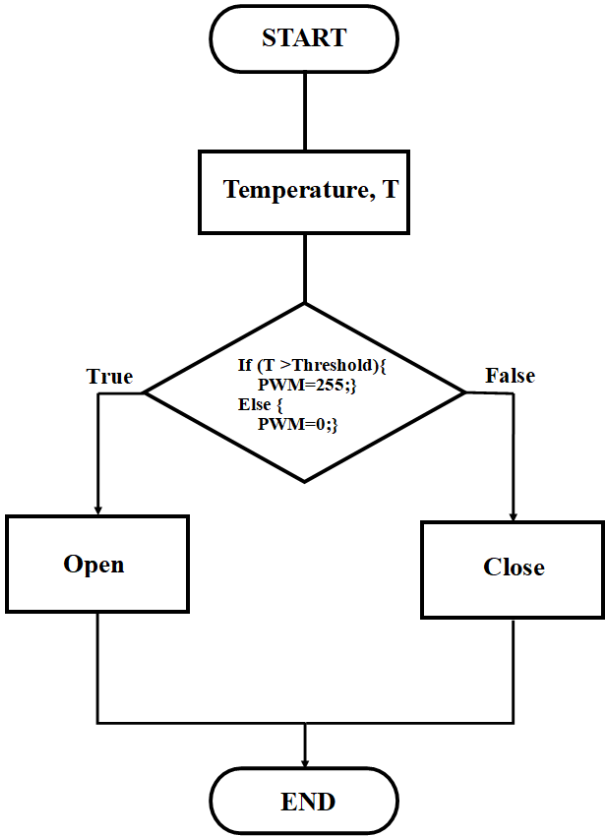

FIGURE 5. The flow diagram of the water dispenser in the cooling system.

The Heat Transfer with Surface-to-Surface Radiation interface couples radiative heat exchange with conduction and convection, which is critical for accurately representing the heating effect of concentrated solar radiation and its dissipation through the cooling medium.

Boundary conditions and assumptions: The inlet boundary condition specifies a constant flow rate corresponding to an average velocity of $78.63\,\mathrm{cm\,s^{-1}}$.

The outlet assumes zero gauge pressure with a fully developed outflow. Ambient air is modelled with fixed temperature (20 °C) and standard atmospheric pressure (1 atm). The intensity of solar radiation varies in the simulation scenarios from 1 to 10 suns ($1\,\text{sun} = 1\,000\,\text{W}\,\text{m}^{-2}$) with the sunlight incident perpendicular to the solar cell surface to represent realistic concentrated solar conditions. The primary objective of the simulation is to quantify the transient heating and cooling rates of the solar cell under these standard external conditions. No wind or forced convection is considered externally; only radiation and natural convection within the system geometry affect the heat transfer balance. The walls of the radiator are assumed to have constant thermal properties, and the material emissivity and reflectivity are defined according to standard values for copper and aluminium.

Numerical solution: The computational mesh is generated with a refined resolution near the fluid-solid interfaces to capture thermal gradients and flow development accurately. The transient solution is computed using a time-dependent solver, capturing the dynamic cooling process from the initial heating to steady temperature stabilisation.

This modelling approach assumes an ideal thermal contact between the copper tubes and the aluminium radiator and neglects possible thermal losses due to imperfect thermal interfaces. It also does not include micro-scale effects such as turbulent eddies, because laminar flow is assumed due to the relatively low flow velocity and small channel dimensions.

Figure 6 illustrates the overall simulation workflow, highlighting the main stages, from geometry creation to multiphysics coupling and numerical post-processing. This comprehensive modelling approach provides a consistent framework for analysing the thermal performance of the proposed active water-cooling system under various solar irradiance levels and design configurations. The numerical results and a discussion of the system's cooling effectiveness and temperature uniformity are presented in the following section.

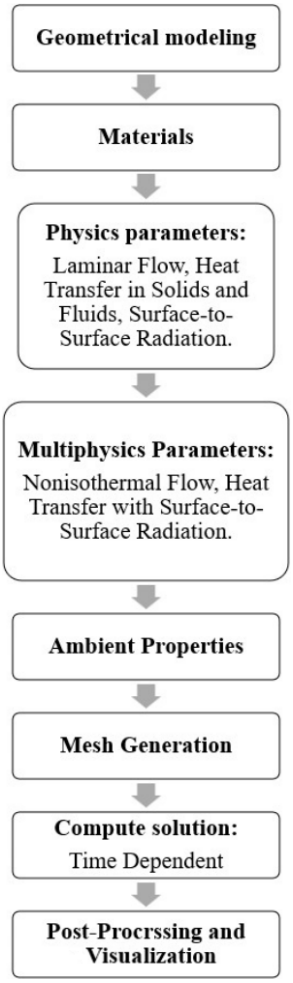

Figure 6. COMSOL Multiphysics simulation algorithm.

2.1. Thermal-electrical relationship

In the context of low-concentration photovoltaic (LCPV) systems, controlling the cell surface temperature is critical for maintaining optimal power output and preventing efficiency losses. Although this study focuses primarily on the thermal performance of the proposed active water-cooling system, it is essential to understand the theoretical link between the cell temperature and the electrical power output. The actual electrical power output of a PV module under real operating conditions can be expressed as [39–41]:

$$P_{\text{PV}} = P_{\text{STC}} \left[1 + \beta_p \left(T_{\text{cell}} - T_{\text{STC}}\right)\right] \frac{H_t}{H_{\text{STC}}}, \quad (1)$$

where, P_{STC} is the nominal power output under Standard Test Conditions (STC), H_t is the actual solar irradiance on the PV panel surface, H_{STC} is the standard irradiance under STC (typically $1\,000\,\text{W}\,\text{m}^{-2}$), T_{cell} is the PV cell surface temperature, T_{STC} is the cell temperature under STC (25 °C), and β_p is the temperature coefficient of power (typically negative for crystalline silicon cells).

A key aspect of this formulation is the accurate estimation of the cell surface temperature T_{cell}, which significantly affects the real power output and the efficiency losses due to thermal effects. An empirical approach for estimating T_{cell} is commonly used, such as the relation proposed in [42]:

$$T_{\text{cell}} = T_\infty + 7.8 \times 10^{-2} H_t, \quad (2)$$

where, T_∞ is the ambient air temperature. This emphasises that higher solar irradiance, in the absence of effective cooling, directly results in higher cell temperatures, leading to a measurable decrease in electrical efficiency.

3. Simulation results of the cooling system

This section shows the results which were obtained using methods described in the previous section. The

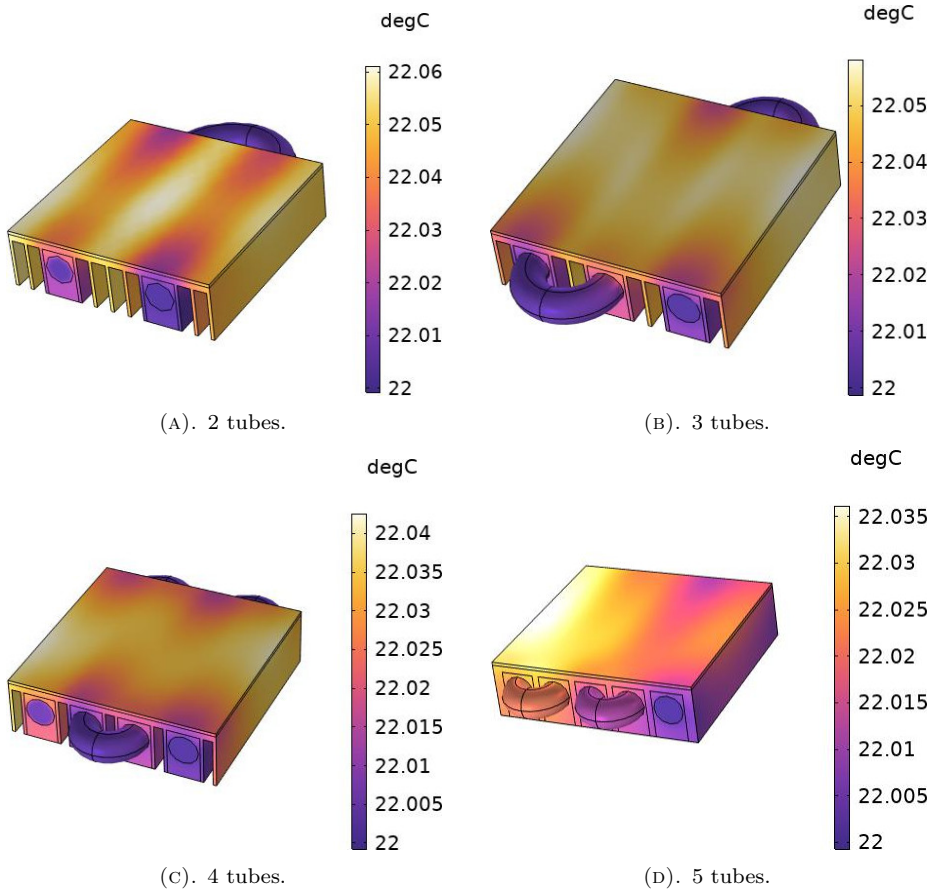

(A). 2 tubes. (B). 3 tubes.

(C). 4 tubes. (D). 5 tubes.

FIGURE 7. Cooling process at solar radiation of 2 suns and number of tubes: 2, 3, 4, and 5 tubes.

cooling process model and cooling time were obtained, and the temperature drop at different concentration ratios was compared. During the computer simulation, solar radiation values of 2 sun and 5 sun, which are included in the low concentration degree, were selected. During the simulation, radiators exposed to concentrated light are cooled from about 40 °C to about 22 °C. The reason for choosing 40 °C as the upper limit is that in real conditions, in the technical documentation of polycrystalline solar cells, the 40 °C limit is indicated as the maximum temperature, and it is known that the degradation of solar cells increases at higher limits.

3.1. Non-uniform temperature of the surface of the solar cell

To fully cool down the solar cell, it is necessary that the water goes through the whole surface of the solar cell. The cooling process was carried out with solar radiation of 2 suns, as a result, we were able to monitor the temperature uniformity on the radiator surface during the cooling process (Figure 7). The radiator cooled from around 40 °C to around 22 °C.

Figure 7 shows the temperature differences on the surface of the radiator at the point when the temperature change stabilises in radiators with different numbers of tubes with solar radiation of 2 suns.

Figure 8 shows that the radiator temperature decreased from about 40 °C to about 22 °C for 5 sun solar radiations. The temperature differences on the surface of the radiators are shown for when the temperature inside the radiators is stabilised.

As can be seen from the results shown in the pictures above, the temperature difference on the surface of the radiator is within 1 °C. We also noticed that the temperature difference varies depending on the number of tubes in the radiator and the amount of solar radiation.

3.2. Cooling time of the solar cells

The next important step in the experiment is to study the cooling rate of the radiators, because the surface temperature of the solar cell increases rapidly when it is exposed to concentrated light. Therefore, a quick response from the cooling system is important.

Results shown in Figure 9 and Figure 10 illustrate the time required to cool down a single solar cell at concentration levels of 2 suns and 5 suns using different numbers of tubes. The number of tubes directly affects the cooling rate. When five tubes are used, the temperature decreases almost twice as fast compared to the system with only two tubes. As mentioned above, depending on the width of the reflective surfaces, the concentration ratio (CR) of the concentrating optics may vary, therefore, it is important to investigate how the temperature changes at different CR values. The

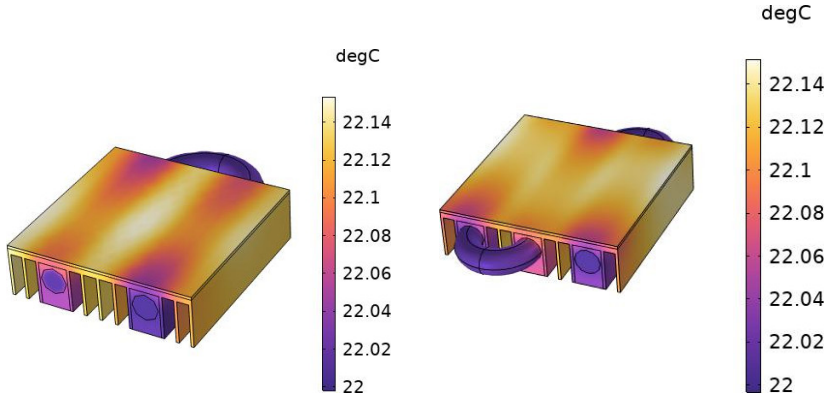

(A). 2 tubes.

(B). 3 tubes.

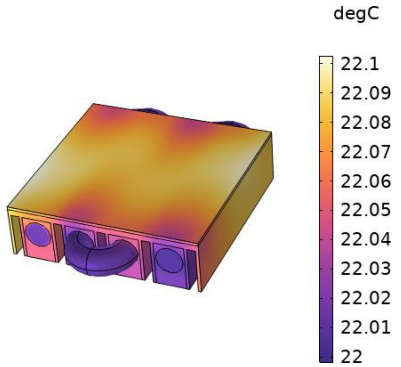

(C). 4 tubes.

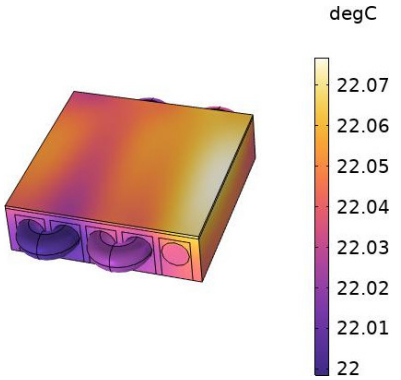

(D). 5 tubes.

Figure 8. Cooling process at solar radiation of 5 suns and number of tubes: 2, 3, 4, and 5 tubes.

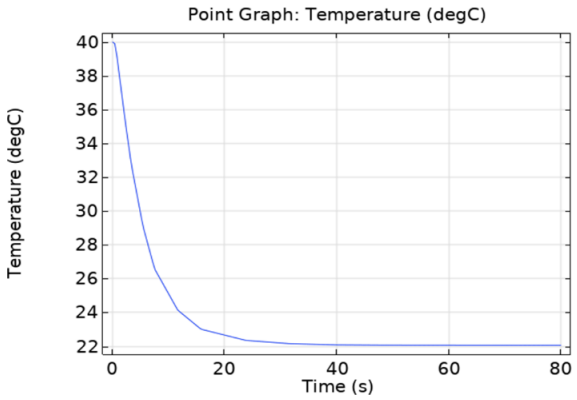

(A). 2 tubes.

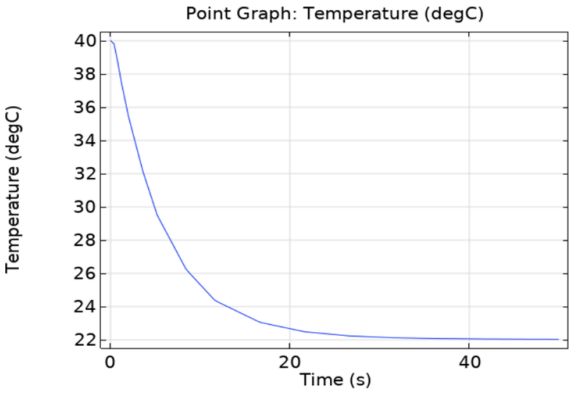

(B). 3 tubes.

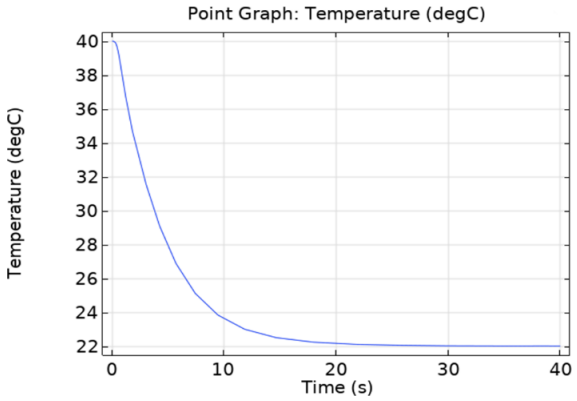

(C). 4 tubes.

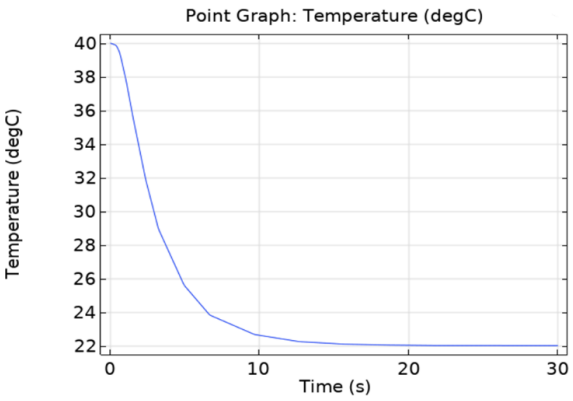

(D). 5 tubes.

Figure 9. Solar cell temperature dependence on time and number of tubes for solar radiation of 2 suns: 2, 3, 4, and 5 tubes.

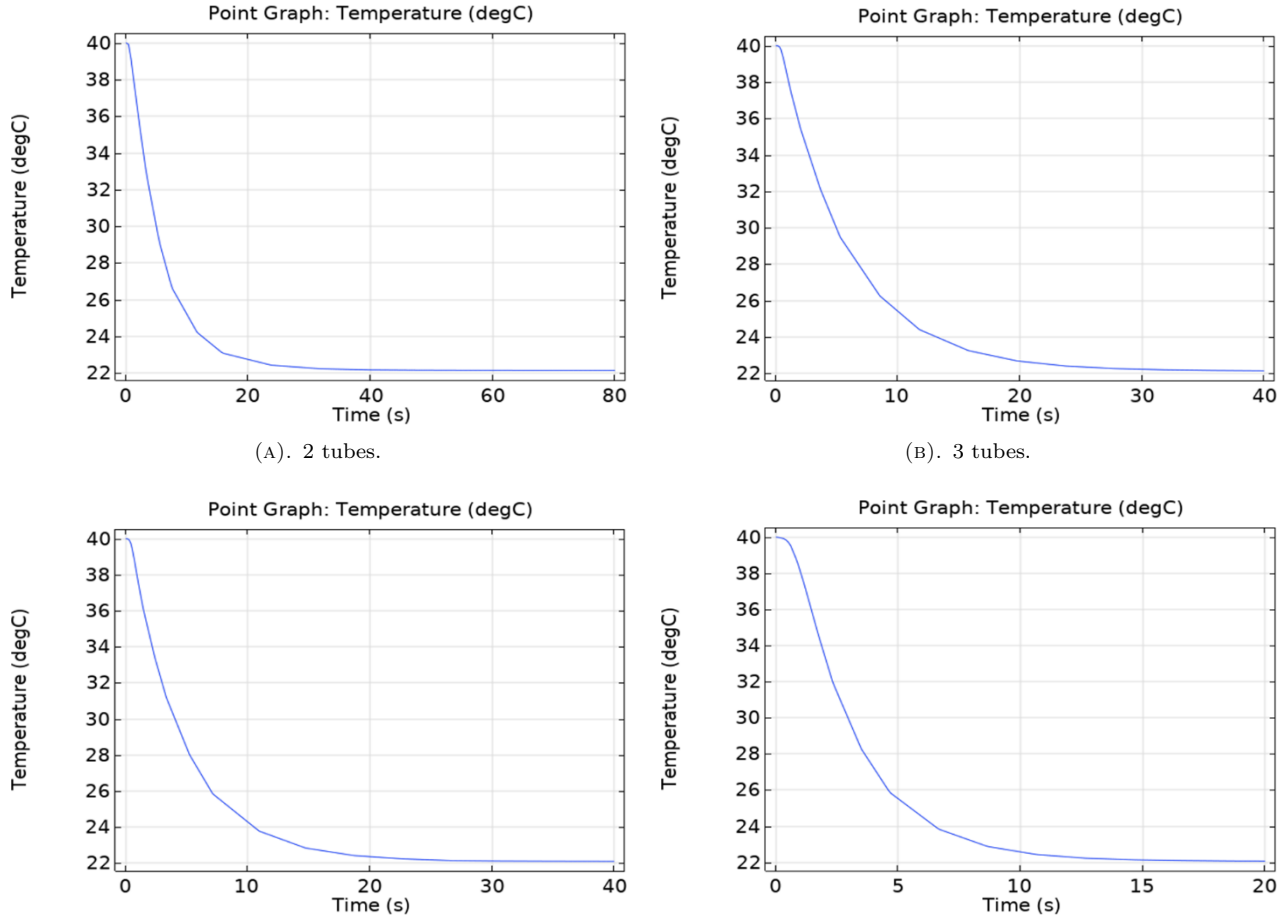

(A). 2 tubes. (B). 3 tubes.

(C). 4 tubes. (D). 5 tubes.

FIGURE 10. Solar cell temperature dependence on time and number of tubes for solar radiation of 5 suns: 2, 3, 4, and 5 tubes.

temperature increases with the increase in solar radiation [43]. The cooling system cools in approximately the same time in both cases, despite the higher solar radiation at 5 suns. During the cooling process, the temperature drops to 22–23 °C within 10 seconds, and thermal equilibrium is established after 15 seconds. These results confirm that the cooling system can provide rapid cooling and maintain the temperature at a level that ensures optimal operating conditions for the solar cell. Figure 11 shows the dependence of the cooling time from 40 °C to 22 °C at different percentages of the maximum water flow rate.

The cooling times of the radiators, from about 40 °C to about 22 °C, varied with solar radiation levels of 2 and 5 suns. The main factors causing these differences are the number of tubes in the radiator and the intensity of solar radiation. The greater the number of tubes, the larger the contact area between the coolant and the heated surface, resulting in more active and efficient heat transfer. Based on the analysis of the results, it can be concluded that the most effective number of tubes for the radiator in this cooling system is five. As the number of tubes increases, cooling becomes faster and the temperature is distributed more evenly across the radiator surface.

3.3. CONNECTING RADIATORS TO EACH OTHER

In addition, cooling radiators for nine solar cells within the Π-shaped optical system can be interconnected in several configurations: 1 input – 1 output, 3 inputs – 3 outputs, and 9 inputs – 9 outputs. The way the radiators are connected affects the overall cooling time of the system, making it important to organise the interconnections efficiently to maintain effective cooling of the active solar cells.

Figure 12 shows the temperature differences on the surface of the radiators for the different connection configurations. In Figure 12a, the radiators are connected in series, so a temperature difference is observed between the radiators: the water entering the first radiator is progressively heated as it passes through each subsequent radiator, resulting in a temperature difference of about 1 °C across the surfaces. In Figure 12b, the water is supplied through three radiators in parallel and then fed onward, showing a similar temperature difference of about 1 °C. Figure 12c demonstrates that when the water is supplied individually to each radiator (9 inputs – 9 outputs), the cooling process is more uniform and the temperature difference across the radiator surfaces decreases to approximately 0.3 °C. This means that among the

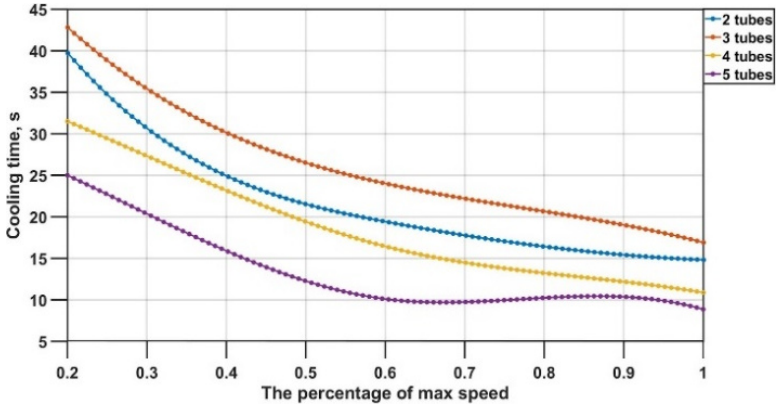

(a). 2 sun.

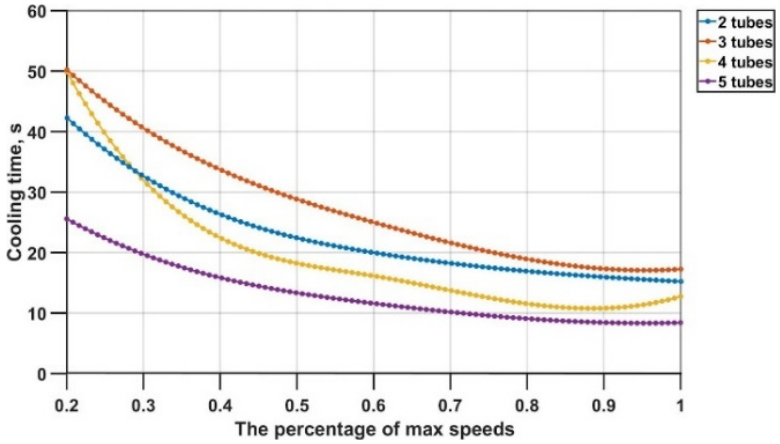

(b). 5 suns.

Figure 11. Dependence of cooling time on different percentages of maximum water flow.

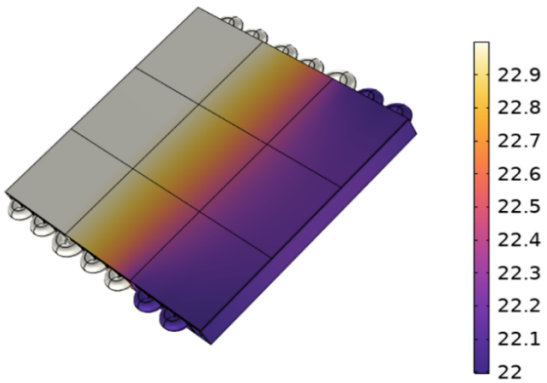

(a). 1 input – 1 output.

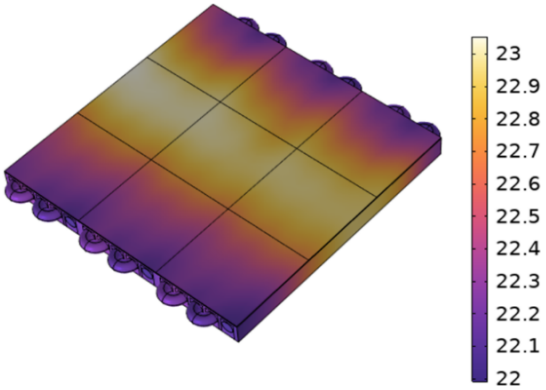

(b). 3 inputs – 3 outputs.

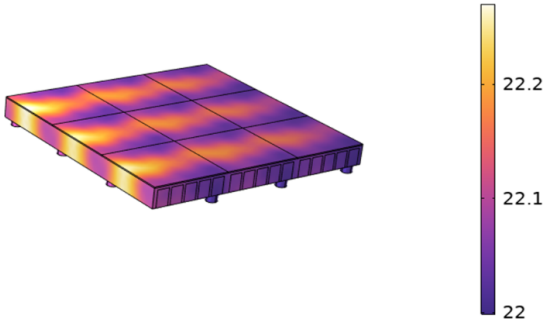

(c). 9 inputs – 9 outputs.

Figure 12. Temperature differences for radiators with different connections.

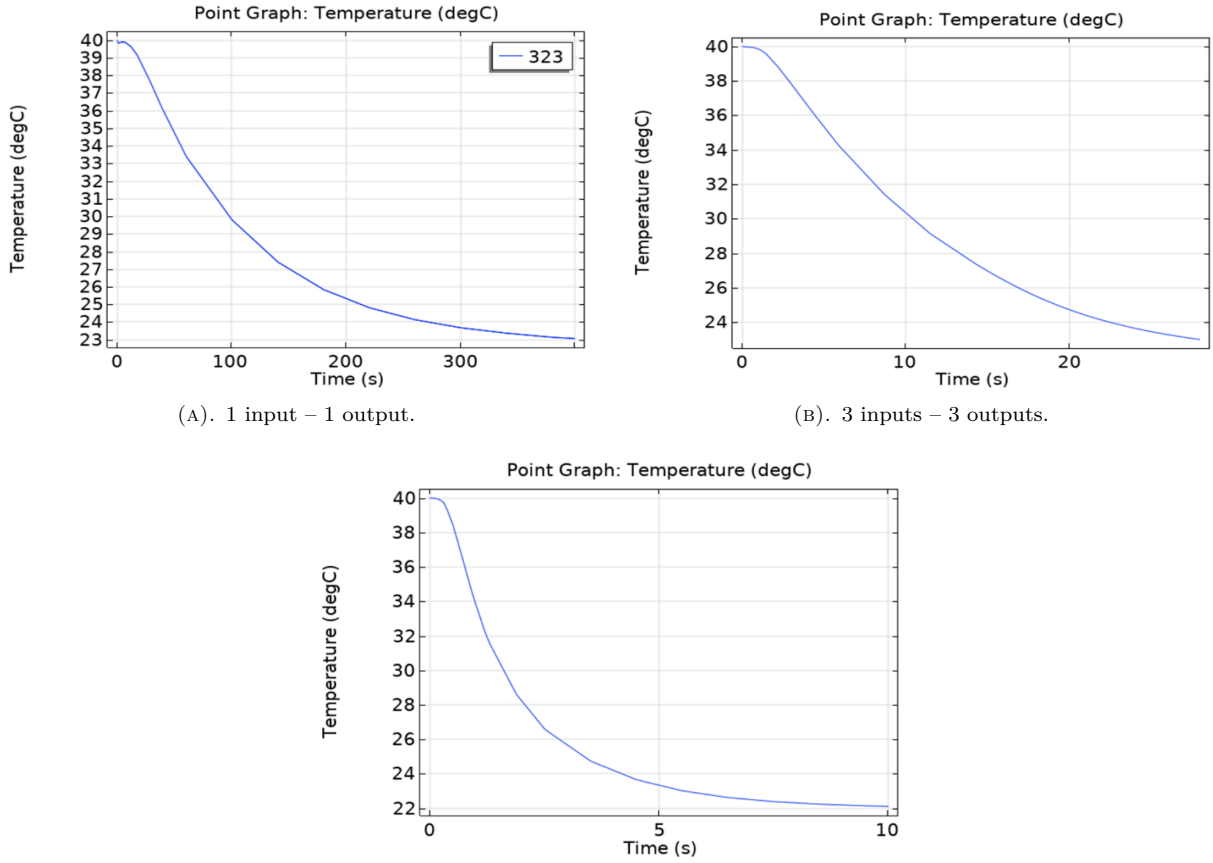

(A). 1 input – 1 output.

(B). 3 inputs – 3 outputs.

(C). 9 inputs – 9 outputs.

FIGURE 13. Time dependence of temperature for different connections of radiator tubes.

three configurations, the 9-input – 9-output version achieves the highest temperature uniformity.

Additionally, the time dependence of the temperature during the cooling process was analysed to determine which configuration provides the fastest cooling (Figure 13).

Figure 13a shows that for the series connection (1 input – 1 output), the temperature drops from 40 °C to about 23 °C in 323 seconds and does not reach 22 °C at all. Figure 13b shows that with the 3-input – 3-output configuration, the temperature reaches 23 °C in 28 seconds, which is a significant improvement. Figure 13c demonstrates that the 9-input – 9-output version decreases the temperature to 22 °C in just 10 seconds – about three times faster than the previous version – and achieves the target condition. In summary, the 9-input – 9-output configuration provides the most efficient and high-performance cooling among the options analysed.

4. Conclusion

A cooling system for a Π-shaped LCPV module was designed and its performance was simulated using the COMSOL Multiphysics platform. The cooling strategy and simulation procedure were described in detail. One of the key advantages of the proposed system is that it does not require a water pump, as water flows by gravity from a certain height, reducing the energy consumption and system complexity. The temperature uniformity and cooling time of radiators with different numbers of tubes were analysed. The results show that for a radiator with five tubes, the temperature difference between the hottest and coolest points was only 0.07 °C, with the cell temperature dropping from 40 °C to 22 °C within 10 seconds. These characteristics have a positive effect on the thermal stability and operational reliability of the solar cell.

In addition, different radiator connection schemes for the Π-shaped optical system with nine solar cells were investigated. The 9-input – 9-output configuration achieved a surface temperature difference of only 0.3 °C and a total cooling time of approximately 10 seconds. This configuration allows for the individual control of cooling for each solar cell, which helps reduce unnecessary energy use caused by variations in solar irradiance and optimises the overall operation of the cooling system. In summary, the proposed cooling system demonstrates rapid cooling capability and can maintain cell temperatures within optimal limits, ensuring stable performance and extending the lifetime of the solar cells.

Acknowledgements

This research has been funded by the Science Committee of the Ministry of Science and Higher Education of the Republic of Kazakhstan. (Grant No. AP19574454).

References

[1] T. Tsoutsos, N. Frantzeskaki, V. Gekas. Environmental impacts from the solar energy technologies. *Energy Policy* **33**(3):289–296, 2005. https://doi.org/10.1016/S0301-4215(03)00241-6

[2] A. A. Aminou Moussavou, A. K. Raji, M. Adonis. Strategic modulation of thermal to electrical energy ratio produced from PV/T module. *Acta Polytechnica* **61**(2):313–323, 2021. https://doi.org/10.14311/AP.2021.61.0313

[3] Y. F. Nassar, H. J. El-Khozondar, M. Elnaggar, et al. Renewable energy potential in the State of Palestine: Proposals for sustainability. *Renewable Energy Focus* **49**:100576, 2024. https://doi.org/10.1016/j.ref.2024.100576

[4] H. J. El-Khozondar, F. El-batta, R. J. El-Khozondar, et al. Standalone hybrid PV/wind/diesel-electric generator system for a COVID-19 quarantine center. *Environmental Progress & Sustainable Energy* **42**(3):e14049, 2023. https://doi.org/10.1002/ep.14049

[5] Y. F. Nassar, S. Y. Alsadi, H. J. El-Khozondar, et al. Design of an isolated renewable hybrid energy system: A case study. *Materials for Renewable and Sustainable Energy* **11**(3):225–240, 2022. https://doi.org/10.1007/s40243-022-00216-1

[6] Y. F. Nassar, H. J. El-Khozondar, M. M. Khaleel, et al. Design of reliable standalone utility-scale pumped hydroelectric storage powered by PV/wind hybrid renewable system. *Energy Conversion and Management* **322**:119173, 2024. https://doi.org/10.1016/j.enconman.2024.119173

[7] Y. Fathi Nassar, S. Yassin Alsadi. Assessment of solar energy potential in Gaza Strip-Palestine. *Sustainable Energy Technologies and Assessments* **31**:318–328, 2019. https://doi.org/10.1016/j.seta.2018.12.010

[8] A. F. M. Ali, E. M. H. Karram, Y. F. Nassar, A. A. Hafez. Reliable and economic isolated renewable hybrid power system with pumped hydropower storage. In *2021 22nd International Middle East Power Systems Conference (MEPCON)*, pp. 515–520. 2021. https://doi.org/10.1109/MEPCON50283.2021.9686233

[9] M. M G Almihat, M. MTE Kahn. Design and implementation of hybrid renewable energy (PV/wind/diesel/battery) microgrids for rural areas. *Solar Energy and Sustainable Development Journal* **12**(1):71–95, 2023. https://doi.org/10.51646/jsesd.v12i1.151

[10] H. J. El-Khozondar, A. A. Asfour, Y. F. Nassar, et al. Photovoltaic solar energy for street lighting: A case study at Kuwaiti roundabout, Gaza strip, Palestine. *Power Engineering and Engineering Thermophysics* **3**(2):77–91, 2024. https://doi.org/https://doi.org/10.56578/peet030201

[11] A. Kagilik, A. Tawel. Performance analysis of 14 MW grid-connected photovoltaic system. *Solar Energy and Sustainable Development Journal* **4**(1):11–21, 2015. https://doi.org/10.51646/jsesd.v4i1.78

[12] M. M. Rahman, J. Pearce. Modular open source solar photovoltaic-powered DC nanogrids with efficient energy management system. *Solar Energy and Sustainable Development Journal* **13**(1):22–42, 2024. https://doi.org/10.51646/jsesd.v13i1.169

[13] H. El Achouby, M. Zaimi, A. Ibral, E. M. Assaid. New analytical approach for modelling effects of temperature and irradiance on physical parameters of photovoltaic solar module. *Energy Conversion and Management* **177**:258–271, 2018. https://doi.org/10.1016/j.enconman.2018.09.054

[14] E. Muñoz, P. G. Vidal, G. Nofuentes, et al. CPV standardization: An overview. *Renewable and Sustainable Energy Reviews* **14**(1):518–523, 2010. https://doi.org/10.1016/j.rser.2009.07.030

[15] A. Ejaz, H. Babar, H. M. Ali, et al. Concentrated photovoltaics as light harvesters: Outlook, recent progress, and challenges. *Sustainable Energy Technologies and Assessments* **46**:101199, 2021. https://doi.org/10.1016/j.seta.2021.101199

[16] K. Shanks, S. Senthilarasu, T. K. Mallick. Optics for concentrating photovoltaics: Trends, limits and opportunities for materials and design. *Renewable and Sustainable Energy Reviews* **60**:394–407, 2016. https://doi.org/10.1016/j.rser.2016.01.089

[17] A. Zahedi. Review of modelling details in relation to low-concentration solar concentrating photovoltaic. *Renewable and Sustainable Energy Reviews* **15**(3):1609–1614, 2011. https://doi.org/10.1016/j.rser.2010.11.051

[18] N. Xu, J. Ji, W. Sun, et al. Outdoor performance analysis of a 1090× point-focus fresnel high concentrator photovoltaic/thermal system with triple-junction solar cells. *Energy Conversion and Management* **100**:191–200, 2015. https://doi.org/10.1016/j.enconman.2015.04.082

[19] G. Dosymbetova, S. Mekhilef, A. Saymbetov, et al. Modeling and simulation of silicon solar cells under low concentration conditions. *Energies* **15**(24):9404, 2022. https://doi.org/10.3390/en15249404

[20] B. Du, E. Hu, M. Kolhe. Performance analysis of water cooled concentrated photovoltaic (CPV) system. *Renewable and Sustainable Energy Reviews* **16**(9):6732–6736, 2012. https://doi.org/10.1016/j.rser.2012.09.007

[21] M. M. Fouad, L. A. Shihata, E. I. Morgan. An integrated review of factors influencing the perfomance of photovoltaic panels. *Renewable and Sustainable Energy Reviews* **80**:1499–1511, 2017. https://doi.org/10.1016/j.rser.2017.05.141

[22] E. Radziemska. The effect of temperature on the power drop in crystalline silicon solar cells. *Renewable Energy* **28**(1):1–12, 2003. https://doi.org/10.1016/S0960-1481(02)00015-0

[23] I. García, M. Victoria, I. Antón. *Temperature Effects on CPV Solar Cells, Optics and Modules*, chap. 5, pp. 245–292. John Wiley & Sons, Ltd, 2016. https://doi.org/10.1002/9781118755655.ch05

[24] S. Jakhar, M. S. Soni, N. Gakkhar. Historical and recent development of concentrating photovoltaic cooling technologies. *Renewable and Sustainable Energy Reviews* **60**:41–59, 2016. https://doi.org/10.1016/j.rser.2016.01.083

[25] S. Sargunanathan, A. Elango, S. T. Mohideen. Performance enhancement of solar photovoltaic cells using effective cooling methods: A review. *Renewable and Sustainable Energy Reviews* **64**:382–393, 2016. https://doi.org/10.1016/j.rser.2016.06.024

[26] A. Royne, C. J. Dey, D. R. Mills. Cooling of photovoltaic cells under concentrated illumination: A critical review. *Solar Energy Materials and Solar Cells* **86**(4):451–483, 2005. https://doi.org/10.1016/j.solmat.2004.09.003

[27] K. A. Ibrahim, P. Luk, Z. Luo. Cooling of concentrated photovoltaic cells – A review and the perspective of pulsating flow cooling. *Energies* **16**(6):2842, 2023. https://doi.org/10.3390/en16062842

[28] A. Radwan, M. Emam, M. Ahmed. Chapter 2.15 – Comparative study of active and passive cooling techniques for concentrated photovoltaic systems. In I. Dincer, C. O. Colpan, O. Kizilkan (eds.), *Exergetic, Energetic and Environmental Dimensions*, pp. 475–505. Academic Press, 2018. https://doi.org/10.1016/B978-0-12-813734-5.00027-5

[29] S. Nižetić, A. Papadopoulos, E. Giama. Comprehensive analysis and general economic-environmental evaluation of cooling techniques for photovoltaic panels, Part I: Passive cooling techniques. *Energy Conversion and Management* **149**:334–354, 2017. https://doi.org/10.1016/j.enconman.2017.07.022

[30] H. M. S. Bahaidarah, A. A. B. Baloch, P. Gandhidasan. Uniform cooling of photovoltaic panels: A review. *Renewable and Sustainable Energy Reviews* **57**:1520–1544, 2016. https://doi.org/10.1016/j.rser.2015.12.064

[31] M. Xiao, L. Tang, X. Zhang, et al. A review on recent development of cooling technologies for concentrated photovoltaics (CPV) systems. *Energies* **11**(12):3416, 2018. https://doi.org/10.3390/en11123416

[32] G. Dosymbetova, S. Mekhilef, S. Orynbassar, et al. Neural network-based active cooling system with IoT monitoring and control for LCPV silicon solar cells. *IEEE Access* **11**:52585–52602, 2023. https://doi.org/10.1109/ACCESS.2023.3280265

[33] A. B. S. Raj, S. P. Kumar, G. Manikandan, P. J. Titus. An experimental study on the performance of concentrated photovoltaic system with cooling system for domestic applications. *International Journal of Engineering and Advanced Technology (IJEAT)* **3**(6):97–101, 2014.

[34] N. A. S. Elminshawy, M. El-Ghandour, Y. Elhenawy, et al. Experimental investigation of a V-trough PV concentrator integrated with a buried water heat exchanger cooling system. *Solar Energy* **193**:706–714, 2019. https://doi.org/10.1016/j.solener.2019.10.013

[35] A. A. Tarabsheh, S. Voutetakis, A. I. Papadopoulos, et al. Investigation of temperature effects in efficiency improvement of non-uniformly cooled photovoltaic cells. *Chemical Engineering Transactions* **35**:1387–1392, 2013. https://doi.org/10.3303/CET1335231

[36] S. A. Zubeer, O. M. Ali. Performance analysis and electrical production of photovoltaic modules using active cooling system and reflectors. *Ain Shams Engineering Journal* **12**(2):2009–2016, 2021. https://doi.org/10.1016/j.asej.2020.09.022

[37] M. Chaabane, H. Mhiri, P. Bournot. Performance optimization of water-cooled concentrated photovoltaic system. *Heat Transfer Engineering* **37**(1):76–81, 2016. https://doi.org/10.1080/01457632.2015.1042344

[38] S. Orynbassar, D. Almen, S. Mekhilef, et al. Minimum solar tracking system for a Fresnel lens-based LCPV. *Renewable Energy* **237**:121607, 2024. https://doi.org/10.1016/j.renene.2024.121607

[39] A. A. Hafez, Y. F. Nassar, M. I. Hammdan, S. Y. Alsadi. Technical and economic feasibility of utility-scale solar energy conversion systems in Saudi Arabia. *Iranian Journal of Science and Technology, Transactions of Electrical Engineering* **44**(1):213–225, 2020. https://doi.org/10.1007/s40998-019-00233-3

[40] H. Awad, Y. F. Nassar, A. Hafez, et al. Optimal design and economic feasibility of rooftop photovoltaic energy system for Assuit University, Egypt. *Ain Shams Engineering Journal* **13**(3):101599, 2022. https://doi.org/10.1016/j.asej.2021.09.026

[41] K. A. A. Amer, M. A. Irhouma, M. I. Hamdan, et al. Economic-Environmental-Energetic (3E) analysis of photovoltaic solar energy systems: Case study of mechanical & renewable energy engineering departments at Wadi AlShatti University. *Wadi AlShatti University Journal of Pure and Applied Science* **3**(1):51–58, 2025.

[42] Y. F. Nassar, A. A. Salem. The reliability of the photovoltaic utilization in southern cities of Libya. *Desalination* **209**(1):86–90, 2007. https://doi.org/10.1016/j.desal.2007.04.013

[43] M. R. Gomaa, M. Al-Dhaifallah, A. Alahmer, H. Rezk. Design, modeling, and experimental investigation of active water cooling concentrating photovoltaic system. *Sustainability* **12**(13):5392, 2020. https://doi.org/10.3390/su12135392